ChemComm

Accepted Manuscript

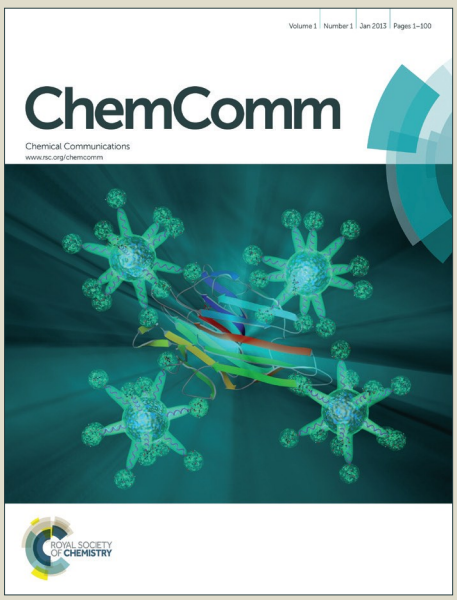

ROYAL SOCIETY OF CHEMISTRY

www.rsc.org/chemcomm

Journal Name

COMMUNICATION

Tuning band alignment by CdS layers using SILAR method to enhance TiO_2/CdS/CdSe quantum-dot solar-cell performance

Received 00th January 20xx,
Accepted 00th January 20xx

DOI: 10.1039/x0xx00000x

www.rsc.org/

Bingkai Zhang,[†a] Jiaxin Zheng,[†a] Xiaoning Li,[†b] Yanyan Fang,[b] Lin-Wang Wang,[a,c] Yuan Lin,*[,a,b] and Feng Pan*[,a]

We report tuning band alignment by optimized CdS layers using SILAR method to achieve the recorded best performance with about 6% PCE in TiO_2/CdS/CdSe QDSSCs. Combined experimental and theoretical study, we find better lattices match between CdS and TiO_2 assists the growth of CdSe, and the combined effect of charge transfer and surface dipole moment at the TiO_2/CdS/CdSe interface shifts the energy levels of TiO_2 upward and increase the solar cell V_{oc}. More importantly, the band gap of CdS buffer layer is sensitive to the distortion induced by lattice mismatch and numbers of CdS layers. For example, barrier for charge transfer disappers with more than 4 layers of CdS, facilitating the charge injection from CdSe to TiO_2.

As an alternative renewable energy source, different kinds of solar cells have been developed in the decades.[1] To improve the efficiency of cells, the design and optimization of interface have played an important role, since photoelectrons separation is closely associated with the kinetics of the electron-transfer processes at the interface.[2,3] As for the quantum-dot sensitized solar cells (QDSSCs), which have attracted much recent interest as a promising photoelectric conversion device due to their tunable adsorption band, high absorption coefficient and multiple exciton effect,[4] an important interface engineering process is to insert a CdS buffer layer between TiO_2 and CdSe in CdSe sensitized anatase-TiO_2 system (TiO_2/CdS/CdSe) to enhance the efficiency of cells. It is generally believed that the presence of CdS buffer layer on one hand promotes the growth of CdSe, and on the other hand facilitates electrons injection from CdSe to TiO_2 by a reorganization of band levels between CdS and CdSe, that is, from type I to type II,[5-7] in which by definition, both the conduction band edge (E_{cb}) and valance band edge (E_{vb}) of CdSe are located in the band gap of TiO_2 in the type I structure, and both the E_{cb} and E_{vb} of CdSe are higher than those of TiO_2 in the type II structure. Nevertheless, the role of CdS buffer layer was still under debate by other experiments. Some suggested CdS buffer layer actually impedes the injection of electrons from CdSe to TiO_2 due to the type-I energy alignment of CdS/CdSe and accelerates charge recombination at the TiO_2/sensitizer interface.[8] The others proposed that the CdS/CdSe quantum dots have a quasi-type-II band alignment with E_{cb} of CdS close to that of CdSe.[9,10] Hence, it is highly desirable to further clarify and get a deep understanding of the role that CdS buffer layer plays in TiO_2/CdS/CdSe cells.

In addition, the optimization of the thickness of CdS buffer layer is also investigated experimentally. Palomares et al.[11] reported that the best cell efficiency for CdS/CdSe co-sensitized TiO_2 system consisting of 6 cycles of CdS and 8 cycles of CdSe. While Lee et al.[12] found 3 cycles of CdS plus 4 cycles of CdSe exhibits the best efficiency. Dai et al.[13] found that the increasing of CdS cycles enhances the short circuit current density. All these experimental findings implied that optimizing the CdS buffer layer is vital to performances of TiO_2/CdS/CdSe cells, but the detailed mechanism is still unclear: what's the relationship between the thickness of the CdS buffer layer and the energy level alignment at the TiO_2/CdS/CdSe interface? How is the electronic structure of the CdS buffer layer tuned by the thickness (successive ionic layer adsorption and reaction (SILAR) cycles), especially within a two-sides confined interface? Such deep insights would not only be helpful for the future interface design to improve the photovoltaic performance but also be of fundamental interest for science.

Herein, we constructed the TiO_2/CdS/CdSe cells with CdS buffer layer deposited on TiO_2 through SILAR method,[14] and tested their photovoltaic performance by varying CdS buffer layer by controlling the SILAR cycles. Figs. 1a and 1b show a

[a] Address here. School of Advanced Materials, Peking University Shenzhen Graduate School, Shenzhen 518055, China. E-mail: panfeng@pkusz.edu.cn (F.P)
[b] Beijing National Laboratory for Molecular Sciences, Key Laboratory of Photochemistry, Institute of Chemistry, Chinese Academy of Sciences, Beijing 100190, China. linyuan@iccas.ac.cn (Y.L)
[c] Materials Science Division, Lawrence Berkeley National Laboratory, Berkeley, California 94720, USA.
† These authors contributed equally to this work.
Electronic Supplementary Information (ESI) available: [details of any supplementary information available should be included here]. See DOI: 10.1039/x0xx00000x

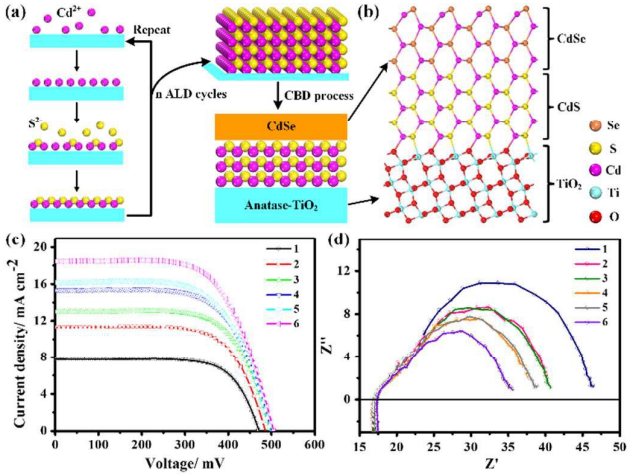

Fig. 1 (a) Schematic of the formation of CdS buffer layer on mesoporous anatase-TiO_2 film via SILAR process. (b) Schematic construction of TiO_2/CdS/CdSe configuration. (c) and (d) *J-V* characteristics and EIS spectra of TiO_2/(CdS)n/CdSe solar cells at different number of CdS cycles (n) measured in the light under zero V bias, respectively. The number after labels denotes the cycles of CdS buffer layer deposition.

schematic diagram of the preparation process of TiO_2/CdS/CdSe QDSSCs and a schematic struction of each material and related interafaces of TiO_2/CdS/CdSe, respectively. For comparison, we also tried to prepare the TiO_2/CdSe by using the chemical bath deposition (CBD) method and found CdSe hardly grows on the TiO_2 film. Then, the thickness optimization of TiO_2 film and CdSe were processed and the details are depicted in the section 1 of Supporting Information (SI). Using the optimized thickness of TiO_2 film and CdSe, we further prepared the TiO_2/CdS/CdSe quantum-dot cells. The *J-V* characteristics of TiO_2/(CdS)n/CdSe cells (Fig. 1c and Table S1 and S3) show the current (J_{sc}) and power conversion efficiency (PCE%) increases more than double with the number of CdS cycles. For example, J_{sc} is increased from 7.77 to 18.47 mA/cm^2, while PCE is raised from 2.6% to 5.94% vs. n=1 to 6 layers of CdS. In contrast, the open circuit voltage (V_{oc}) increases from 465 mV to 505mV and fill factor (FF) decreases from 0.72 to 0.64 vs. n=1 to 6 layers of CdS, respectively, which means that both V_{oc} and FF change much less significantly vs. CdS layers. The higher V_{oc} suggests that the E_{cb} of TiO_2 shifts upward with the increasing number of CdS cycles. The lower FF is probably because of the low diriving force for the electron injection with the cycle of CdS. The E_{cb} of CdS shifts downward with the increasing number of CdS cycles. The higher PCE of TiO_2/(CdS)6/CdSe is attributed to its broader light adsorption range wich leads to a higher J_{sc} compared with that of the TiO_2/(CdS)1/CdSe. In addition, PCE and related all factors (J_{sc}, V_{oc}, FF) almost keep constant after more than 6 layers of CdS (See Table S4). The best performing device had an efficiency of about 6% (5.9-6.3% in different experiments), which is higher than other CdS/CdSe sensitized solar cells prepared in the same type[15-18] and is similar to the latest report (6.01 %) in which CdS/CdSe are co-sensitized on TiO_2 nanowire-coated hollow spheres[19]. The electrochemical impedance spectroscopy (EIS) measurements of the cells (Fig. 1d) show that the conductivity of TiO_2/(CdS)n/CdSe cells are increased by the CdS cycles. The above observations implied that CdS layers with increasing cycles may broaden light adsorption and reduce energy barrier for excited electron injection from CdSe layer to TiO_2.

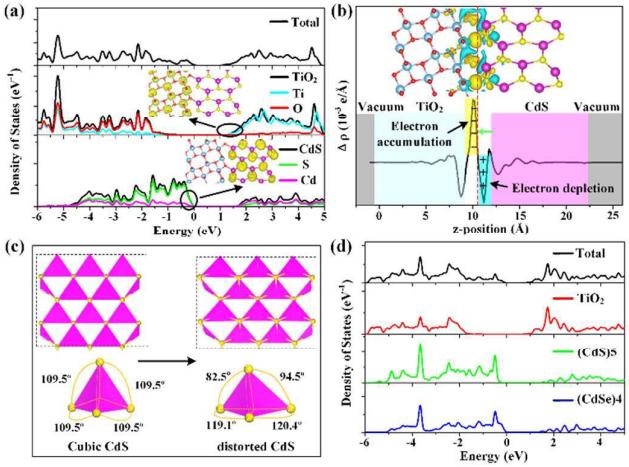

Fig. 2 (a) TDOS and PDOS of TiO_2/(CdS)5. Inset shows the charge states in the energy range 0.00-0.50 eV below E_{vb} and above E_{cb} of TiO_2/CdS. (b) Charge density differences heterojunction and the corresponding planar average of the induced charge density difference for TiO_2/CdS. The yellow (cyan) region represents charge accumulation (depletion). (c) Distortion of CdS layer from the cubic structure of bulk structure to distorted tetrahedral structure near heterojunction interface. (d) TDOS and PDOS of TiO_2/CdS/CdSe composites.

In addition, *J-V* curves also suggest that the voltage first increases with increasing CdS cycles and then comes to a saturation afer 3 cycles of CdS layer (Fig. 1c), indicating that the band levels of CdS layer can be tuned by its cycles from higher to lower levels. So questionsarise: (i) From the point of quantum-dot crystal growth, how the insertion of CdS buffer layer promotes the growth of CdSe; (ii) from the point of tuning eletronic structure, how the insertion of CdS layers with TiO_2/(CdS)n/CdSe quantum-dots affects their energy levels, and how does the number of CdS buffer layers by controlling SILAR cycles affect the band gap and alignment? To answer these questions, we did a comprehensive study on the TiO_2/CdS/CdSe interfacial properties using DFT method in the following part.

The most important step is to establish a reasonable interface structure between anatase-TiO_2 and CdS for studying the TiO_2/CdS/CdSe composites. As depicted in Fig. 1a, for the CdS layer grown by SILAR on anatase-TiO_2, the TiO_2/CdS/CdSe samples were investigated by means of TEM analyses (Fig. S6). We found the (101) plane of TiO_2 and (110) plane of CdSe are the most exposed surfaces, respectively, which are consistent with previous studies.[20,21] Therefore, the (101) surface of TiO_2 is chosen as the substrate. Based on the (2 × 2) supercell

parameters of TiO_2(101) (10.87 × 7.73 Å^2), we found the nonpolar (110) face of cubic CdS, a (2 × 2) supercell (11.65 × 8.24 Å^2) to match best with TiO_2(101) surface (the lattice mismatch less than 7%). Thus, the (110) surface of cubic CdS and CdSe are chosen as the contact surface according to the best lattice matching at the interface. While the mismatch between CdSe(110) (12.11 × 8.56 Å^2) and TiO_2(101) is beyond 11%, suggesting the growth of CdSe on TiO_2 is difficult. The current results are consistent with experimental observation which suggests CdS grow on TiO_2 film more easily.[8] Figs. 1b, S1a and S1b show the interface bonded with the chemical bond (O-Cd) between O atom TiO_2 of and Cd of CdS in the optimized structures of TiO_2/CdS/CdSe and TiO_2/CdS, respectively. After relaxation, the average bond distance O-Cd is 2.38 Å, which is close to that of bulk Cd-O (2.34 Å), indicating a strong interaction between CdS and TiO_2 surfaces.

In the second step, we examined the geometric and electronic structures of TiO_2/(CdS)n and TiO_2/(CdS)n/CdSe by selecting 5 layers of CdS as typical model as below. Fig. 2a shows the total or project density of states (TDOS or PDOS) of TiO_2/(CdS)5 system, and the charge distributions of the states in the band edges are shown in Fig. 2a. It can be found that the E_{vb} of CdS is lower than that of TiO_2 and the E_{cb} of CdS is higher than that of TiO_2, indicating that the band alignment of TiO_2/CdS system belongs to the type-II structure with both E_{vb} and E_{cb} of CdS locates higher in energy level than those of TiO_2. As a result, the electrons generated in CdS are energetically favorable to be transferred into TiO_2 and holes are transferred into CdS. From charge distribution, it is clear that there is little charge localized in the O-Cd bonding interface, implying charge recombination at the interface seems unfavorable. The band edge states are delocalized in bulk TiO_2 and bulk CdS, which is consistent with the prediction of the DOS results. In addiiton, there is no interfacial gap states, and charges could be readily transferred across the interface under visible-light irradiation. Fig. 2b shows the three-dimensional charge density diverence by subtracting the electronic charge of a TiO_2/CdS composite from those of the CdS and TiO_2 structures and the charge redistribution along the z-direction normal to the interface. The planar-averaged charge density diverence along the z direction also exhibits charge redistribution. The positive (negative) values represent electron accumulation (depletion). It was found that the electrons are transferred from CdS to TiO_2, and more specifically, the electrons are transferred from Cd atoms to O atoms. Therefore, an interface dipole was generated with a direction from CdS side to TiO_2 side. After further checking the structure properties of the TiO_2/CdS, it was found that, after relaxation, TiO_2 remain the bulk TiO_2-like structure but CdS induces a structural distortion. As depicted in Fig. 2c, the lattice mismatch at the interface leads to CdS structure change from the cubic to a distorted tetrahedral. Compared with the cubic CdS, the average bond distance of Cd-S in tetrahedral is lengthened from 2.562 Å to 2.635 Å, and such stress may affect its electronic structures. Besides, the DOS and PDOS of the TiO_2/(CdS)5/CdSe are also calculated as shown in Fig. 2d, in which CdSe grains are constructed through isomorphic replacement of the surface S atoms by Se atoms in a reconstructed four Cd-S layers since CdS/CdSe is a homojunction. The energy levels of TiO_2/CdS and CdS/CdSe

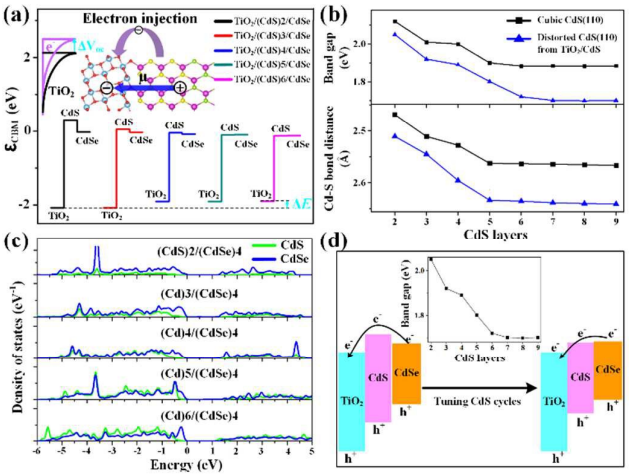

Fig. 3 (a) The E_{cb} energy of TiO_2, CdS, and CdSe respect to their core potential energy in TiO_2/(CdS)n/CdSe. The inset is schematic of dipoles effect. (b) Energy gap of cubic and distorted CdS(110) surfaces as a function of CdS cycles. (c) PDOS of TiO_2/(CdS)n/(CdSe)4 with different CdS cycles. (d) Schematic of band alignment of TiO_2/(CdS)n/CdSe by tuning layers (n).

suggested by Fig. 2d exhibit a Type-II and a quasi-Type-II structure, respectively. In the quasi-Type-II structure of CdS/CdSe, the E_{cb} of CdS is close to that of CdSe but E_{vb} of CdS is lower than that of CdSe. Therefore, the energy levels by insertion of CdS layers may not impede the charge transfer, just as the experimental observation and previous experimental works indicating[5, 6]. Furthermore, the calculated electrostatic potential of the interface, deducing electron transport route based on electrostatic potential difference shown in Fig. S8 (SI), also agrees well the DOS analysis.

Hence, the energy levels of TiO_2, CdS, and CdSe are assessed by aligning the E_{cb} energy with respect to their core potential energy, repectively. First, on one hand, as mentioned in Fig. 2b, the charge transfer from CdS to TiO_2 generates a dipole field at the heterojunction interface (inset of Fig. 3a), which leads to downward shift of the the conduction band of TiO_2. Such interface dipoles inducing energy levles shifts have also been reported in other solar-cell systems.[22,23] On the other hand, the accumulation of electrons in TiO_2 shifts the conduction band of TiO_2 upward.[24-27] Thus, the shift of TiO_2 conduction band is determined by the combined effect of charge transfer and surface dipole moment. To shed light on this issue, the E_{cb} of TiO_2/(CdS)n/CdSe (n = 2-6) is shown in Fig. 3a. It was found that the E_{cb} of TiO_2 raises with the increasing thickness of CdS layer, because the dipole potential diminishes. The increased extent of $E_{cb}(TiO_2)$ is labed as ΔE as shown in Fig. 3a. The increase of $E_{cb}(TiO_2)$ is beneficial to the cell V_{oc}. Fig. 3a also suggests that the E_{cb} difference between CdS and TiO_2 reduces with the increasing CdS cycles, which would reduce the diriving force for the electron injection. These results agrees with the experimental observation as

shwon in Fig. 1c and Table S1. Second, band gaps can be tuned by the number of CdS layers in both ideal cubic CdS (from ideal CdS crystal structure) with vacuum as interface and the distorted tetrahedral CdS structure near the heterojunction interface shown in Fig. 2c and 3b, in which all band gaps first decrease rapidly with increasing CdS layers, and then to a nearly invariable value after 5-6 layers. This is bacause as the layers increase, the outlayers of CdS would suffer less stress from the interface and possess a more relaxed state. The enlarged Cd-S bonds suggest a weaker interaction between Cd and S atoms with the increasing cycles, which would make electrons become more delocalized and itinerant, thus to narrow the band gap. The simialr results are also found in TiO_2/PbS interface, it was shown that TiO_2 surface structure induces PbS bond angle distortions which changed the energy gap of the PbS QDs at the interface.[28] Thus, the band gap reduction (vs. n=1 to 6 layer) affects the light adsorption range, resulting in high PCE and J_{sc}, as shown in Fig. 1c and Table S1. And above 6 layers, the band gap invariant is consistent with the tiny change of photovoltaic parameters as shown in Table S4.

Therefore, the transition of energy levels from TiO_2 to CdSe can be tuned by interface dipole and band gap of CdS buffer, which can be controlled by SILAR cycles. Insight of the CdS layers vs. band energy levels of TiO_2/CdS/CdSe was further examined by analysizing the PDOS of TiO_2/(CdS)n/CdSe with different CdS layers, as shown in Fig. 3c, which shows that CdS buffer layer serves as a barrier for charge transfer when the layers are under 4. Interestingly, the barrier disappers when the layers are 4 (n=4) and more than 4 (n>4), which would lead to facilitate the charge injection from CdSe to TiO_2. Therefore, tuning CdS buffer layers by SILAR cycles to optimize the energy levels of TiO_2/CdS/CdSe quantum-dot can tune the band alignment to enhance the solar-cell performance as shown in Fig. 3d.

In summary, the role of CdS buffer layer played in the TiO_2/CdS/CdSe was investigated based on experiments and theoretical calculations. The combined effect of charge transfer and dipole moment at TiO_2/CdS/CdSe heterojunction interface produces an upward energy levels shift for TiO_2. Besides, charges could be readily transferred across the interface under visible-light irradiation due to the absence of interfacial gap states. Most important of all, the band gap of CdS buffer layer can be tuned by varying its number of layers, which were controllably formed by SILAR process. Electrons could not be efficiently transferred when the CdS buffer layer is too thin (e.g. less than 4 layers of CdS), and tuning the layers of CdS can induce a suitable energy level alignment between CdS and CdSe (e.g. thicker than 4 layers of CdS). As a result, the reorganization of energy levels with band alignment between TiO_2 and CdSe by insertion of optimized CdS buffer layer forms a stepwise structure of band-edge levels to benefit photoelectrons separation to enhance solar-cell performance. These findings provide insight for design of high performance solar-cells with optimized buffer layers.

Acknowledgements

This work was supported by Guangdong Innovation Team Project (No. 2013N080) and Shenzhen Science and Technology Research Grant (peacock plan KYPT20141016105435850).

Notes and references

1 B. Petter Jelle, C. Breivik and H. Drolsum Røkenes, *Solar Energy Materials and Solar Cells*, 2012, **100**, 69-96.
2 J. Zheng, K. Zhang, Y. Fang, Y. Zuo, Y. Duan, Z. Zhuo, X. Chen, W. Yang, Y. Lin, M. S. Wong and F. Pan, *ACS Applied Materials & Interfaces*, 2015, **7**, 25341-25351.
3 M. Logar, S. Xu, S. Acharya and F. B. Prinz, *Nano Letters*, 2015, **15**, 1855-1860.
4 J. H. Bang and P. V. Kamat, *Advanced Functional Materials*, 2010, **20**, 1970-1976.
5 T. Toyoda, K. Oshikane, D. Li, Y. Luo, Q. Meng and Q. Shen, *Journal of Applied Physics*, 2010, **108**, 114304.
6 Y.-L. Lee and Y.-S. Lo, *Advanced Functional Materials*, 2009, **19**, 604-609.
7 H.-M. Cheng, K.-Y. Huang, K.-M. Lee, P. Yu, S.-C. Lin, J.-H. Huang, C.-G. Wu and J. Tang, *Physical Chemistry Chemical Physics*, 2012, **14**, 13539-13548.
8 M. A. Hossain, J. R. Jennings, C. Shen, J. H. Pan, Z. Y. Koh, N. Mathews and Q. Wang, *Journal of Materials Chemistry*, 2012, **22**, 16235-16242.
9 C. She, A. Demortière, E. V. Shevchenko and M. Pelton, *The Journal of Physical Chemistry Letters*, 2011, **2**, 1469-1475.
10 A. Sitt, F. D. Sala, G. Menagen and U. Banin, *Nano Letters*, 2009, **9**, 3470-3476.
11 T. Zewdu, J. N. Clifford, J. P. Hernández and E. Palomares, *Energy & Environmental Science*, 2011, **4**, 4633-4638.
12 Y. L. Lee and Y. S. Lo, *Advanced Functional Materials*, 2009, **19**, 604-609.
13 Y. Zhang, J. Zhu, X. Yu, J. Wei, L. Hu and S. Dai, *Solar Energy*, 2012, **86**, 964-971.
14 A. F. Palmstrom, P. K. Santra and S. F. Bent, *Nanoscale*, 2015, **7**, 12266-12283.
15 C. Chen, M. Ye, M. Lv, C. Gong, W. Guo and C. Lin, *Electrochimica Acta*, 2014, **121**, 175-182.
16 L. Chen, L. Tuo, J. Rao and X. Zhou, *Materials Letters*, 2014, **124**, 161-164.
17 Z. Pan, H. Zhang, K. Cheng, Y. Hou, J. Hua and X. Zhong, *ACS Nano*, 2012, **6**, 3982-3991.
18 J. H. Park, D. H. Kim, S. S. Shin, H. S. Han, M. H. Lee, H. S. Jung, J. H. Noh and K. S. Hong, *Advanced Energy Materials*, 2014, **4**, 1300395.
19 Y.-F. Xu, W.-Q. Wu, H.-S. Rao, H.-Y. Chen, D.-B. Kuang and C.-Y. Su, *Nano Energy*, 2015, **11**, 621-630.
20 X.-Q. Gong, A. Selloni, M. Batzill and U. Diebold, *Nat Mater*, 2006, **5**, 665-670.
21 H. Zhang, B. Chen, J. F. Banfield and G. A. Waychunas, *Physical Review B*, 2008, **78**, 214106.
22 S. Rühle, M. Shalom and A. Zaban, *ChemPhysChem*, 2010, **11**, 2290-2304.
23 N. Yaacobi-Gross, M. Soreni-Harari, M. Zimin, S. Kababya, A. Schmidt and N. Tessler, *Nat Mater*, 2011, **10**, 974-979.
24 J. M. Azpiroz, E. Ronca and F. De Angelis, *The Journal of Physical Chemistry Letters*, 2015, **6**, 1423-1429.
25 J. M. Azpiroz, I. Infante and F. De Angelis, *The Journal of Physical Chemistry C*, 2015, **119**, 12739-12748.
26 M. Kazes, S. Buhbut, S. Itzhakov, O. Lahad, A. Zaban and D. Oron, *The Journal of Physical Chemistry Letters*, 2014, **5**, 2717-2722.
27 S. Buhbut, S. Itzhakov, I. Hod, D. Oron and A. Zaban, *Nano Letters*, 2013, **13**, 4456-4461.
28 O. Trejo, K. E. Roelofs, S. Xu, M. Logar, R. Sarangi, D. Nordlund, A. L. Dadlani, R. Kravec, N. P. Dasgupta, S. F. Bent and F. B. Prinz, *Nano Letters*, 2015, **15**, 7829-7836.